Submitted, accepted and published by
Mitigation and Adaptation Strategies for Global Change (2019)
https://doi.org/10.1007/s11027-019-9840-5

Biomass combustion by Chemical Looping with Oxygen Uncoupling process: experiments with Cu-based and Cu-Mn mixed oxide as oxygen carriers

Iñaki ADÁNEZ-RUBIO[1,2], Antón PÉREZ-ASTRAY[1], Alberto ABAD[1], Pilar GAYÁN[1*], Luis F. DE DIEGO[1], Juan ADÁNEZ[1]

[1] *Instituto de Carboquímica (ICB-CSIC), Miguel Luesma Castán 4, 50018 Zaragoza, Spain*

[2] *Aragón Institute of Engineering Research (I3A), Dept. of Chemical and Environmental Engineering, University of Zaragoza, Zaragoza 50018*

**Corresponding Author, pgayan@icb.csic.es*

Abstract –CCS combined with biomass as fuel (BECCS) opens the possibility to reach negative CO_2 emissions, which implies removing CO_2 already emitted to the atmosphere. Chemical Looping Combustion (CLC) with biomass can be considered as a promising new BECCS technology as CLC has low cost and energy penalty. In CLC, the oxygen needed for combustion is supplied by a solid oxygen carrier circulating between the fuel and air reactors. In the fuel reactor, the fuel is oxidized producing a CO_2-concentrated stream while the oxygen carrier is reduced. In the air reactor, the oxygen carrier is regenerated with air. Chemical Looping with Oxygen Uncoupling (CLOU) is a CLC technology that allows the combustion of solid fuels as in common combustion with air by means of using oxygen carriers that release gaseous oxygen in the fuel reactor. In last years, several Cu-based, Mn-based and mixed oxides oxygen carriers have been tested showing good CLOU properties. Among them, Cu-based and Cu-Mn mixed oxides show high reactivity, O_2 release rate and high O_2 equilibrium concentration. The aim of this work is to study the viability of biomass combustion by CLOU process. The combustion of three types of biomass (pine sawdust, olive stone and almond shell) are studied in a continuous 1.5 kW_{th} CLC unit. Two oxygen carriers were tested: a Cu-based oxygen carrier with $MgAl_2O_4$ as an inert prepared by spray drying (Cu60MgAl) and a mixed Cu-Mn oxide prepared by spray granulation (Cu34Mn66). These materials are capable of releasing gaseous oxygen when they are reduced in a different range of temperatures. CO_2 capture and combustion efficiency were evaluated. Two fuel reactor operation temperatures were used: 775-850 ºC for Cu34Mn66 and 900-935 ºC for Cu60MgAl. High CO_2 capture efficiencies and 100% combustion efficiency were reached with both oxygen carriers and with all the biomasses tested. With Cu34Mn66, a 98% of CO_2 capture efficiency was reached at a low temperature as 850ºC burning pine sawdust. Using the same fuel, but with Cu60MgAl as oxygen carrier, 100% of CO_2 capture efficiency at 935ºC in the fuel reactor was obtained. Reasons of the different behavior are analyzed.

Submitted, accepted and published by
Mitigation and Adaptation Strategies for Global Change (2019)
https://doi.org/10.1007/s11027-019-9840-5

1 Introduction

According to the Paris Agreement (2015) (IPCC 2014), in order to limit the global temperature increase to 2 ºC or less it is necessary to decrease CO_2 emissions to the atmosphere and even to reach negative CO_2 emissions during this century. Carbon Capture and Storage (CCS) technologies allow CO_2 capture from large stationary combustion sources. If waste biomass is used in these processes as fuel then these technologies can be considered as Bioenergy with Carbon Capture and Storage (BECCS) technologies. Biomass is a CO_2 neutral fuel. Therefore, BECCS technologies allow actually removing CO_2 from the atmosphere making the negative CO_2 emissions concept possible.

One of the CCS technologies with lower energy penalty and cost associated to CO_2 capture is Chemical Looping Combustion (CLC). The basic principle behind CLC is the avoidance of contact between fuel and air during the combustion process. Therefore, inherent CO_2 capture in the process is obtained. In CLC, the oxygen needed for combustion is supplied by a solid oxygen carrier, normally a metal oxide, circulating between two interconnected reactors: the fuel and air reactors. In the fuel reactor, the fuel is burned to CO_2 and H_2O while the oxygen carrier is reduced. The reduced oxygen carrier is then transferred to the air reactor where it is reoxidized in air before a new cycle begins. Figure 1 shows a scheme of the CLC process for solid fuels. When solid fuels are used as fuel in CLC it is possible that a part of unconverted char being transferred to the air reactor with the reduced oxygen carrier, decreasing the CO_2 capture process. To avoid this, it could be necessary to use a carbon stripper that allows the separation of the unconverted char from the oxygen carrier and to recirculate it to the fuel reactor. Also, if the gases of the fuel combustion are not fully burned to CO_2 and H_2O, decreasing the combustion efficiency, it would be necessary fully convert the fuel reactor outlet gases. Thus allowed using an oxygen polishing step downstream from the fuel reactor, see Figure 1. Certain oxygen carriers are able to release gaseous oxygen while they are reduced. This is known as Chemical Looping with Oxygen Uncoupling (CLOU). The gaseous oxygen is able to burn the volatiles and char generated once the solid fuel has been introduced into the fuel reactor.

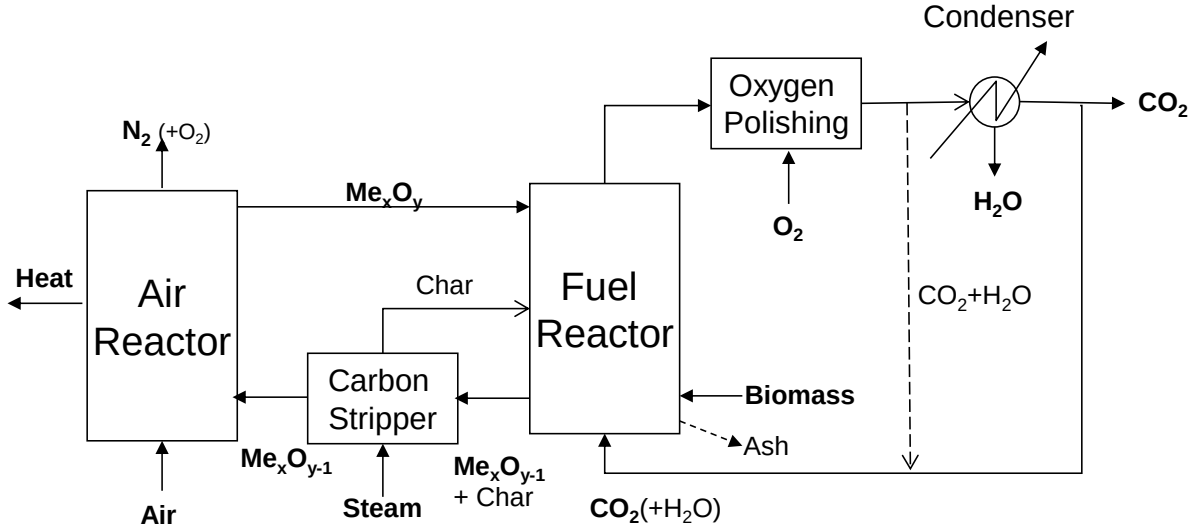

Figure 1. Scheme of the Chemical Looping Combustion (CLC) process for solid fuels.

One of the main differences of the CLOU process respect to the CLC is the oxygen carrier, which is able to generate O_2 (g) at the operating conditions. This gaseous oxygen improves

Submitted, accepted and published by
Mitigation and Adaptation Strategies for Global Change (2019)
https://doi.org/10.1007/s11027-019-9840-5

the kinetic of combustion of volatile matter and char from the solid fuel by gas-gas and gas-solid reactions, (Abad et al. 2012), see reactions (1)-(4).

$$2Me_XO_Y \Leftrightarrow 2Me_XO_{Y-1} + O_2 \quad (1)$$

$$Solid\ fuel \Rightarrow Volattile\ matter + Char \quad (2)$$

$$Volatile\ matter + O_2 \Rightarrow CO_2 + H_2O \quad (3)$$

$$Char + O_2 \Rightarrow CO_2 + Ash \quad (4)$$

Only a few oxides have the adequate characteristic to be used in CLOU process (CuO/Cu_2O; Mn_2O_3/Mn_3O_4 and Co_3O_4/CoO) (Mattisson et al. 2009). Cu-based oxygen carriers have faster oxygen release than Mn-based oxides and the operational temperature is higher than that for Mn and Co-based oxides.

The feasibility of CLC of biomass under CLOU mode was already demonstrated by Adánez-Rubio et al. (Adánez-Rubio et al. 2014a; Adánez-Rubio et al. 2018b; Mendiara et al. 2016) using Cu-based or Cu-Mn mixed oxide oxygen carriers. In these works, high CO_2 capture and combustion efficiencies were reached. A perovkite oxygen carrier ($CaMn_{0.9}Mg_{0.1}O_{3-\delta}$) was used by Schmitz and Linderholm, using as fuel a very low sulphur biochar in a 10 kW_{th} unit (Schmitz and Linderholm 2016). They observed high combustion efficiencies and CO_2 capture efficiencies higher than 98%. Moreover, Wang et al. (Wang et al. 2017) used a Cu supported on olivine oxygen carrier (38 wt% of CuO) burning batches of pine sawdust in a batch fluidized bed reactor. They obtained a 99.3% of CO_2 capture efficiency at 950 ºC, together with unburnt products in the gas stream. The aim of this work is to compare the behaviour of two oxygen carriers, a Cu-based and a Cu-Mn mixed oxide, in the combustion of different kind of biomasses. Both oxygen carriers have been previously tested with different solids fuels, mainly coals. In the case of the Cu-based oxygen carrier, it was tested with coal and char coal in a batch fluidized bed reactor (Adánez-Rubio et al. 2012a), and with coals of different ranks in a continuous CLOU unit (Abad et al. 2012; Adánez-Rubio et al. 2013; Adánez-Rubio et al. 2014b). On the other hand, for the Cu-Mn mixed oxide also was tested with coal and char coal in a batch fluidized bed reactor (Adánez-Rubio et al. 2017b); and with different rank coals in a continuous CLOU unit (Adánez-Rubio et al. 2018a; Adánez-Rubio et al. 2017a).

2 Experimental

2.1 Materials

Two oxygen carriers have been studied in the biomass combustion by CLOU process. On the one hand, a Cu-based oxygen carrier prepared by spray drying manufactured by VITO (Flemish Institute for Technological Research, Belgium) using $MgAl_2O_4$ as inert material. The CuO content was 60 wt%. Particles were calcined for 24 h at 1100ºC. From now on the oxygen carrier was named as Cu60MgAl. Reaction (5) describes the release of gaseous oxygen by the oxygen carrier. On the other hand, a Cu-Mn mixed oxide prepared by spray granulation in a spouted fluidized bed system at ICB-CSIC was also used as oxygen carrier. The CuO content of particles was 34 wt% and a 66 wt% was Mn_3O_4. The particles were calcined 2 h at 1125 ºC. From now on the oxygen carrier was named as Cu34Mn66.The active

Submitted, accepted and published by
Mitigation and Adaptation Strategies for Global Change (2019)
https://doi.org/10.1007/s11027-019-9840-5

phase in the mixed oxide was $Cu_{1.5}Mn_{1.5}O_4$. Reaction (6) describes the release of gaseous oxygen by every oxygen carrier.

$$2\ CuO \leftrightarrow Cu_2O + ½\ O_2 \quad (5)$$

$$2\ Cu_{1.5}Mn_{1.5}O_4 \leftrightarrow 3\ CuMnO_2 + O_2 \quad (6)$$

Table 1 shows the main properties of both oxygen carriers. The particle size used was +100-300 μm.

Table 1. Properties of the oxygen carriers used in this work.

	Cu60MgAl	Cu34Mn66
Experimental Oxygen transport capacity, R_{OC} (wt%)	6.0	4.0
Crushing strength (N)	2.4	1.9
Skeletal density (kg/m^3)	4600	4100
Porosity (%)	16.1	12.0
Specific surface area, BET (m^2/g)	< 0.5	< 0.5
XRD main phases	CuO, $MgAl_2O_4$	$Cu_{1.5}Mn_{1.5}O_4$, Mn_3O_4

Three different biomasses were combusted during the experimental campaign with the oxygen carrier. Pine sawdust (Pinus sylvestris) is commonly used as a reference biomass because of its large use and distribution. Two different agricultural residues were also used and compared with the pine sawdust, almond shell (Prunus dulcis) and olive stone (Olea europaea). They were selected considering their annual production (Council 2017; Fruit 2017). Raw materials were dried and sieved to +500–2000 μm. Properties of the three biomasses are shown in Table 2.

Table 2. Properties of the biomasses used in this work.

	Pine sawdust	Almond shell	Olive stone
Proximate Analysis (wt%)			
Moisture	4.2	2.3	9.4
Volatile matter	81.0	76.6	72.5
Fixed carbon	14.4	20.0	17.3
Ash	0.4	1.1	0.8
Ultimate Analysis (wt%)			
C	51.3	50.2	46.5
H	6.0	5.7	4.8
N	0.3	0.2	0.2
S	0.0	0.0	0.0
O*	37.8	40.5	38.3
LHV (kJ/kg)	19158	18071	17807
Ω_{SF} (kg O_2/kg biomass)	1.5	1.4	1.2

*Calculated by difference

2.2 Experimental set-up

A schematic view of the experimental set-up is shown in Figure 2. The set-up was basically composed of two interconnected fluidized bed reactors –the air and fuel reactors– joined by a

Submitted, accepted and published by
Mitigation and Adaptation Strategies for Global Change (2019)
https://doi.org/10.1007/s11027-019-9840-5

loop seal, a riser for solids transport from the air reactor to the fuel reactor, a cyclone and a solids valve to control the solids circulation flow rate in the system. A diverting solids valve located below the cyclone allowed the measurement of the solids circulation flow rates at any time. Therefore, this design allowed to control and to measure the solids circulation flow rate between both reactors.

The fuel reactor consisted of a bubbling fluidized bed with 5 cm of inner diameter and 20 cm bed height. The fuel reactor was fluidized with N_2 for an accurate analysis of the results. The gas flow was 250 L_N/h, corresponding to a gas velocity of ~ 0.15 m/s at 900 ºC. Biomass was fed by a screw feeder at the bottom of the bed just above the fuel reactor distributor plate in order to maximize the time that the fuel and volatile matter are in contact with the bed material. A small N_2 flow (24 L_N/h) was introduced in the initial part of the screw feeder to avoid any possible reverse gas flow. The oxygen carrier was reduced in the fuel reactor and burned the fuel. Reduced oxygen carrier particles overflowed into the air reactor through a U-shaped fluidized bed loop seal with 3 cm of inner diameter, to avoid gas mixing between fuel and air. A N_2 flow of 90 L_N/h was introduced in the loop seal.

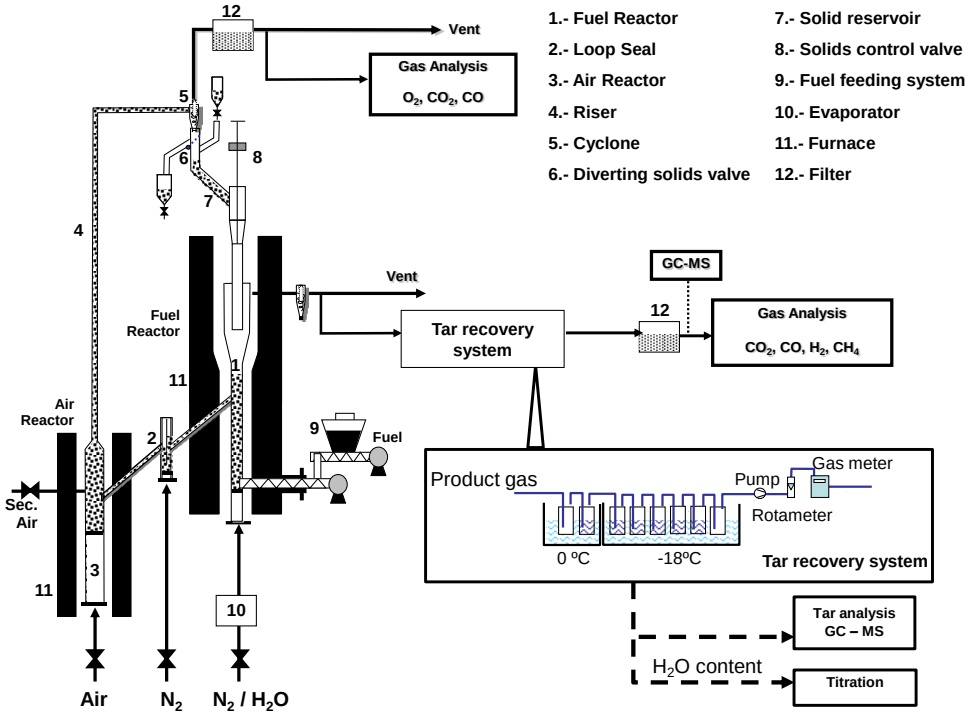

Figure 2. Schematic view of the ICB-CSIC-s1 unit.

The oxidation of the carrier took place in the air reactor, consisting of a bubbling fluidized bed with 8 cm of inner diameter and 10 cm bed height, and followed by a riser. The air flow was 2100 L_N/h. In addition, a secondary air flow (600 L_N/h) was introduced at the top of the bubbling bed to help particle entrainment. N_2 and unreacted O_2 left the air reactor passing through a high-efficiency cyclone and a filter before the stack. The oxidized solid particles recovered by the cyclone were sent to a solids reservoir, setting the oxygen carrier ready to start a new cycle. In addition, these particles act as a loop seal avoiding the leakage of gas between the fuel reactor and the riser. The regenerated oxygen carrier particles returned to the fuel reactor by gravity from the solids reservoir through a solids valve which controlled the flow rate of solids entering the fuel reactor.

The total oxygen carrier inventory in the system was 3 kg, being about 1 kg in the fuel reactor. CO, CO_2, H_2, CH_4 and O_2 concentration in the fuel reactor outlet and also CO, CO_2 and O_2 from the air reactor were continuously recorded. For CH_4, CO and CO_2 a nondispersive infrared (NDIR) analyser (Siemens Ultramat 23) was used; a paramagnetic

Submitted, accepted and published by
Mitigation and Adaptation Strategies for Global Change (2019)
https://doi.org/10.1007/s11027-019-9840-5

analyser (Siemens Ultramat 23 and Oxymat 6) was used for O_2 concentration measurement and a thermal conductivity detector (Siemens Calomat 6) was used for H_2. The collection of tar at the fuel reactor outlet was done according to the standard tar protocol (Simell et al. 2000).

2.3 Experimental Planning

Table 3 shows a compilation of the main variables used in each test. With the oxygen carrier Cu60MgAl a total of 10 h of operation were carried out without agglomeration. With the Cu34Mn66 oxygen carrier a total of 65 h of hot fluidization conditions whereof 40 h with biomass combustion with the same batch of oxygen carrier particles were carried out.

Table 3. Main Data for Experimental Tests in the CLOU Prototype

Test	T_{FR} (ºC)	T_{AR} (ºC)	$[O_2]_{inAR}$ (%)	ϕ	$\dot{m}_s$ (kg/h)	$\dot{m}_{SF}$ (kg/h)	Power (W)	m^*_{FR} (kg/MW$_{th}$)
				Cu60MgAl				
P01	**900**	900	21	1.2	4.1	0.22	1200	565
P02	**920**	900	21	1.2	4.1	0.22	1200	565
P03	**935**	900	21	1.2	4.1	0.22	1200	565
				Cu34Mn66				
P04	**775**	800	21	3.9	22.5	0.14	740	1200
P05	**800**	800	21	3.9	22.5	0.14	740	1200
P06	**825**	800	21	3.9	22.5	0.14	740	1200
P07	**850**	800	21	3.9	22.5	0.14	740	1200
A01	**775**	800	21	3.0	20.3	0.173	860	1150
A02	**800**	800	21	3.0	20.3	0.173	860	1150
A03	**825**	800	21	3.0	20.3	0.173	860	1150
A04	**850**	800	21	3.0	20.3	0.173	860	1150
O01	**775**	800	21	3.3	22.5	0.225	1040	760
O02	**800**	800	21	3.3	22.5	0.225	1040	760
O03	**825**	800	21	3.3	22.5	0.225	1040	760
O04	**850**	800	21	3.3	22.5	0.225	1040	760

The oxygen carrier to fuel ratio, ϕ, is defined as the quotient between the oxygen supplied by the oxygen carrier and the oxygen demanded for the complete fuel combustion. The oxygen carrier to fuel ratio (ϕ) was calculated by the following equation:

$$\phi = \frac{\text{Oxygen supply by the oxygen carrier}}{\text{Oxygen demanded by the fuel for full combustion}} \quad (3)$$

To analyse the performance of the CLOU process, the combustion efficiency in the fuel reactor and the CO_2 capture efficiency were calculated. Calculations are based on the molar flow of every gas analysed, F_i, which is determined from the measured concentrations. Mass balances were checked and a closing about 95% was found for the carbon balance.

The combustion efficiency in the fuel reactor was calculated through the ratio between the oxygen required to fully burn unconverted gases (CH_4, CO and H_2) at the fuel reactor exit and

Submitted, accepted and published by
Mitigation and Adaptation Strategies for Global Change (2019)
https://doi.org/10.1007/s11027-019-9840-5

the oxygen demanded by the biomass converted in the fuel reactor. Thus, the oxygen demanded by the carbon bypassed to the air reactor, $F_{CO_2,AR}$, is subtracted to the oxygen demanded by biomass in the denominator. Therefore, the combustion efficiency in the fuel reactor was calculated as:

$$\eta_{comb,FR} = 1 - \frac{4F_{CH_4,outFR} + F_{CO,outFR} + F_{H_2,outFR}}{\frac{1}{M_{O_2}} 2\Omega_{SF}\dot{m}_{SF} - 2F_{CO_2,outAR}} \quad (4)$$

where Ω_{SF} is the stoichiometric mass of O_2 to convert 1 kg of biomass (kg/kg), m_{SF} is the mass-based flow of biomass fed-in to the fuel reactor (kg/s) and M_{O_2} the molecular weight of O_2 (kg/mol).

The CO_2 capture efficiency, η_{CC}, was defined as the fraction of carbon initially present in the biomass fed which is actually at the outlet of fuel reactor as CO_2. This is the actual CO_2 captured in the CLOU system; the rest is exiting together with nitrogen at the air reactor outlet.

$$\eta_{CC} = 1 - \frac{F_{CO_2,outAR}}{F_{CO_2,outFR} + F_{CO,outFR} + F_{CH_4,outFR} + F_{CO_2,outAR}} \quad (5)$$

The char conversion ($X_{char,FR}$) is defined as the fraction of carbon in the char formed in the fuel reactor which is released to the fuel reactor exhaust gas stream (Adánez et al. 2018; Mendiara et al. 2018):

$$X_{Char,FR} = \frac{[F_{CO_2,FR} + F_{CO,FR} + F_{CH_4,FR} - F_{C,vol}]_{out}}{[F_{CO_2,FR} + F_{CO,FR} + F_{CH_4,FR} + F_{CO_2,AR} - F_{C,vol}]_{out}} \quad (6)$$

where $F_{C,vol}$ is the carbon flow coming from the volatile matter.

3 Results

The effect of the temperature in the fuel reactor was analyzed and compared for both oxygen carriers and among the three biomasses. For this purpose, the fuel reactor temperature was varied from 900 to 935 ºC with Cu60MgAl oxygen carrier burning pine sawdust (P01-P03). For Cu34Mn66 the fuel reactor temperature was varied from 775 ºC to 850 ºC for the pine sawdust fuel (P04-P07), the almond shell (A01-A04) and the olive stone (O01-O04).

The gases that exit from the fuel and the air reactors were continuously analyzed. As an example, Figure 3 shows the gas concentration (dry basis) as a function of the operation time in the pine sawdust experiments with Cu34Mn66 oxygen carrier (P04-P07). The fuel reactor temperature varied from 775 to 850 ºC, and each temperature was maintained at steady state around 60 min. It can be seen that, when the fuel reactor temperature varied a transition period around 20 min appears before the new steady state is reached. During the steady state the temperature and the gas concentration were almost maintained as a constant. No unburnt products (CH_4, CO or H_2) were detected at the outlet gases neither at the lower temperature (775 ºC). So, complete combustion of the biomass in the fuel reactor to CO_2 and H_2O was

Submitted, accepted and published by
Mitigation and Adaptation Strategies for Global Change (2019)
https://doi.org/10.1007/s11027-019-9840-5

obtained, and all the volatiles were completely converted in the fuel reactor by the molecular oxygen released by the oxygen carrier. Insignificant tar amounts were found using tar protocol (Simell et al. 2000) for both oxygen carriers.

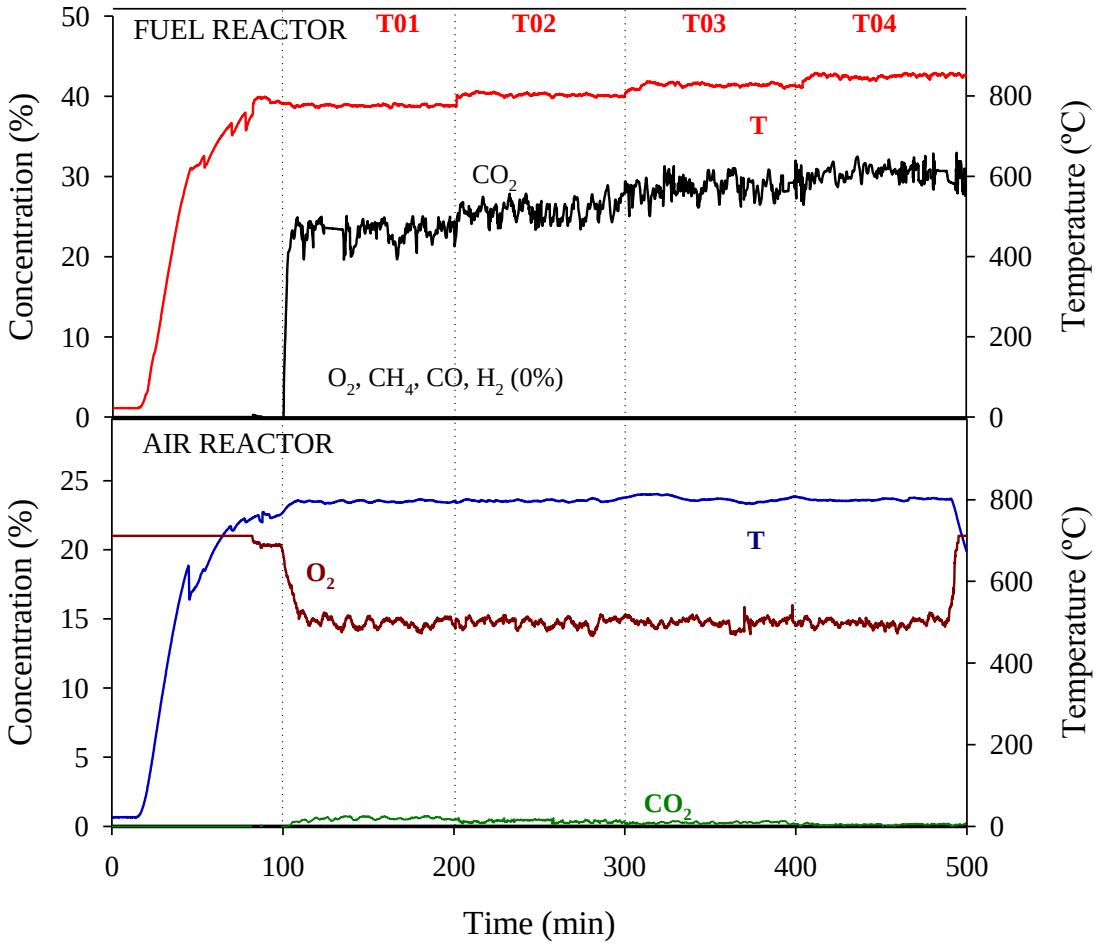

Figure 3. Evolution of the gas composition in the air and fuel reactor as temperature in the fuel reactor was varied. Experimental tests P04-P07. ($\dot{m}_S$) ≈ 22.5 kg/h; ($\dot{m}_{SF}$) ≈ 0.140 kg/h.

It can be seen that an increase in the fuel reactor temperature, results in an increase of the CO_2 concentration in the fuel reactor outlet gas stream. This is because of the increase of char conversion in the fuel reactor that decreased the CO_2 concentration at the air reactor outlet. Also, it can be appreciated that no gaseous oxygen was measured at the exit of the fuel reactor. This was different of what happened in a previous work burning biomass with a Cu-based oxygen carrier (Adánez-Rubio et al. 2014a). This fact could be related with the low fuel reactor temperature together with the high amount of volatiles in the biomass composition. Volatiles in the fuel reactor will consume oxygen released by the oxygen carrier. This issue is highly relevant with biomass due to its high volatile content. Therefore, the oxygen concentration in the fuel reactor outlet could decrease to 0 mainly for the material with a lower oxygen uncoupling capability as is the case of CuMn compared to Cu. However with this oxygen carrier CO_2 and H_2O were the only gases detected in the fuel reactor outlet stream, together with a fraction of the N_2 used as fluidizing agent. Here, it is relevant to say that N_2 was used as fluidizing agent during the experimental campaign in order to allow an accurate calculation of the combustion efficiency

and CO_2 capture parameters. However, the fuel reactor would be fluidized by recirculated CO_2 instead of N_2 at an industrial scale. Thus, CO_2 would not be diluted in N_2, being the CO_2 capture intrinsic to the CLC process. During the biomass combustion it is possible that part of the volatiles generated by the devolatilization of the biomass react directly with the oxygen carrier by CLC reaction. However, most of oxygen would be transferred via oxygen uncoupling because: (1) complete combustion is achieved, which has not possible via gas-solid reaction with solid fuels(Adánez et al. 2018); and (2) char is highly converted even in the absence of a gasification agent in the fluidizing medium(Adánez-Rubio et al. 2012a), being O_2 from the oxygen carrier the gasifying agent. In fact, it was determined that the oxygen uncoupling mechanism prevailed over the gas-solid reaction with materials with this capability, as was the case of CaMn perovskite (Abad et al. 2018).

Respect to the air to fuel ratio in CLOU experiments and considering the design of the experimental CLOU unit, the required air excess is high and, as a consequence, the oxygen concentration at the air reactor exit is about 15 %; see Fig. 3. However, no restrictions on the oxygen carrier regeneration has been observed for the Cu-based material(Adánez-Rubio et al. 2014c), while a slight decrease in the regeneration capability was observed for the CuMn material(Adánez-Rubio et al. 2017b). Anyway, the effect of the air excess with the CuMn material was evaluated in a previous work. It was observed that a decrease in the air excess did not affect negatively to the combustion efficiency, and only a slight decrease in the char conversion was verified (Adánez-Rubio et al. 2018b).

3.1 Combustion efficiency

Taking into account the experiments carried out with Cu60MgAl oxygen carrier, Figure 4 shows the combustion efficiency obtained in the experimental unit as a function of the fuel reactor temperature. Complete combustion of biomass to CO_2 and H_2O was found in the fuel reactor at temperatures higher than 900 ºC. The solids inventory in the fuel reactor was 565 kg/MW_{th} in all tests. Nevertheless, complete combustion can be expected with a lower solids inventory.

In Figure 4, also it can be seen the combustion efficiency as a function of the fuel reactor temperature using Cu34Mn66 oxygen carrier for the three biomasses. Complete combustion of all biomasses to CO_2 and H_2O was obtained for all the temperatures analyzed. It is remarkable that complete combustion was even obtained at a fuel reactor temperature as low as 775 ºC. So, the present work shows that a Cu-Mn-based oxygen carrier is able to obtain complete combustion of the pine biomass even at 775 ºC. This high combustion efficiency at low fuel reactor temperatures was due to the higher O_2 equilibrium concentration of the Cu-Mn mixed oxide ($Cu_{1.5}Mn_{1.5}O_4$) under 900ºC (at 850 ºC 2 vol% for $Cu_{1.5}Mn_{1.5}O_4$ (Adánez-Rubio et al. 2017b) and 0.4 vol% for CuO (Adánez-Rubio et al. 2012b)).

Submitted, accepted and published by
Mitigation and Adaptation Strategies for Global Change (2019)
https://doi.org/10.1007/s11027-019-9840-5

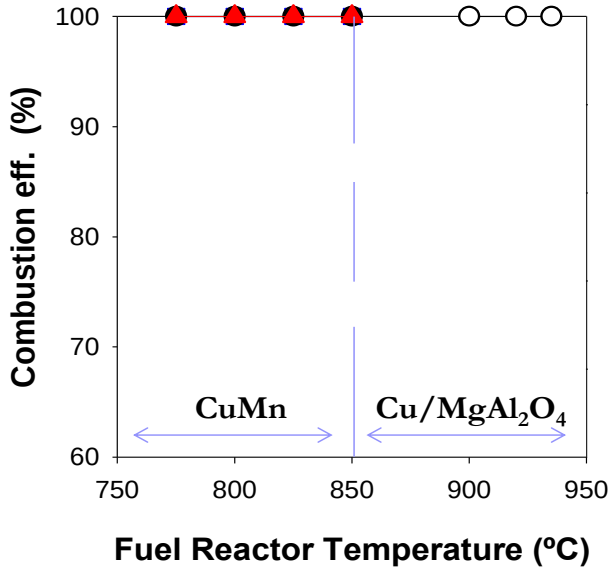

Figure 4. Combustion efficiency in the fuel reactor as a function of the fuel reactor temperature for the experiments carried out with Cu60MgAl and Cu34Mn66 oxygen carriers and three different biomasses: pine sawdust (●,○), almond shell (■) and olive stone (▲).

Figure 5 shows the equilibrium concentration of O_2 as a function of the temperature for the systems CuO/Cu_2O and Mn_2O_3/Mn_3O_4 together the O_2 concentrations measured in batch fluidized bed reactor tests (Adánez-Rubio et al. 2017b), because thermodynamic information on $Cu_{1.5}Mn_{1.5}O_4$ is not available. As in other mixed oxides O_2 concentration is intermediate between those corresponding to the pure metal oxides. Experimental points plotted corresponds to the measured in a zone of near constant concentration

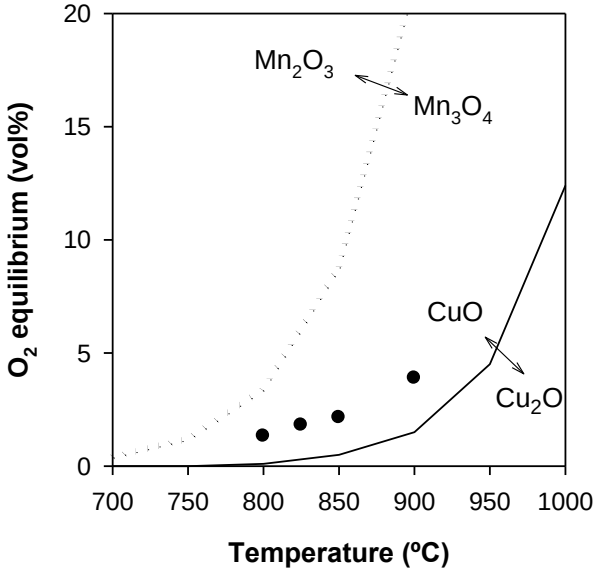

Figure 5. O_2 concentration at equilibrium as a function of the temperature for the systems: (—)CuO/Cu_2O,(-···-) Mn_2O_3/Mn_3O_4 and experimental points obtained for (●) $Cu_{1.5}Mn_{1.5}O_4/CuMnO_2$ (Adánez-Rubio et al. 2017b).

Note that biomass has high volatile matter content, e.g. pine sawdust contains 81% volatile matter. Therefore, even with these high volatile matter contents, the results showed full combustion of the biomasses in all tests in CLOU mode with Cu and Cu-Mn materials. Note

Submitted, accepted and published by
Mitigation and Adaptation Strategies for Global Change (2019)
https://doi.org/10.1007/s11027-019-9840-5

also that unburnt compounds are always present at the outlet of the fuel reactor for materials without oxygen uncoupling properties, even if highly reactive materials or a high solids inventory were used (Garcia Labiano et al. 2013; Gayán et al. 2013). For example, the combustion efficiency of biomass using an iron based oxygen carrier was about $\eta_{comb,FR}$ = 80% with 1550 kg/MW_{th}. This fact highlights the relevance of the oxygen uncoupling process with both Cu-based and Cu-Mn mixed oxide oxygen carriers in order to achieve complete combustion of the fuel by the CLOU process with a low amount of solids.

It can be seen that for both oxygen carriers when the CLOU effect is high enough, complete combustion was obtained in their respective operating temperature windows: 775-850 ºC for Cu34Mn66 and 900-935 ºC for Cu60MgAl, and the need of an oxygen polishing step would be avoided (see Figure 1), which is required using materials without oxygen uncoupling capability (Adánez et al. 2018).

3.2 CO_2 capture efficiency

Focusing on the CO_2 capture efficiency, it depends on the unburnt char transferred to the air reactor, where it is burnt emitting CO_2 to the atmosphere. Figure 6 shows (a) the CO_2 capture efficiency and; (b) the char conversion in the experiments carried out with Cu60MgAl and Cu34Mn66 oxygen carriers. For pine sawdust, Figure 6(a) shows that high CO_2 capture efficiency was obtained in all cases. With temperatures higher than 800 ºC in the fuel reactor the CO_2 capture efficiencies were higher than 90%. Also, it can be seen the positive effect on the CO_2 capture efficiency of the fuel reactor temperature, reaching a value of 98% at 850 ºC with Cu34Mn66 and 100% of capture with Cu60MgAl at 935ºC. This is because of the fact that the CO_2 capture efficiency is directly related with the char conversion and its reactivity, see Figure 6(b). The more char conversion in the fuel reactor, the lower amount of unburnt char is transferred to the air reactor and released to the atmosphere (Adánez-Rubio et al. 2018b).

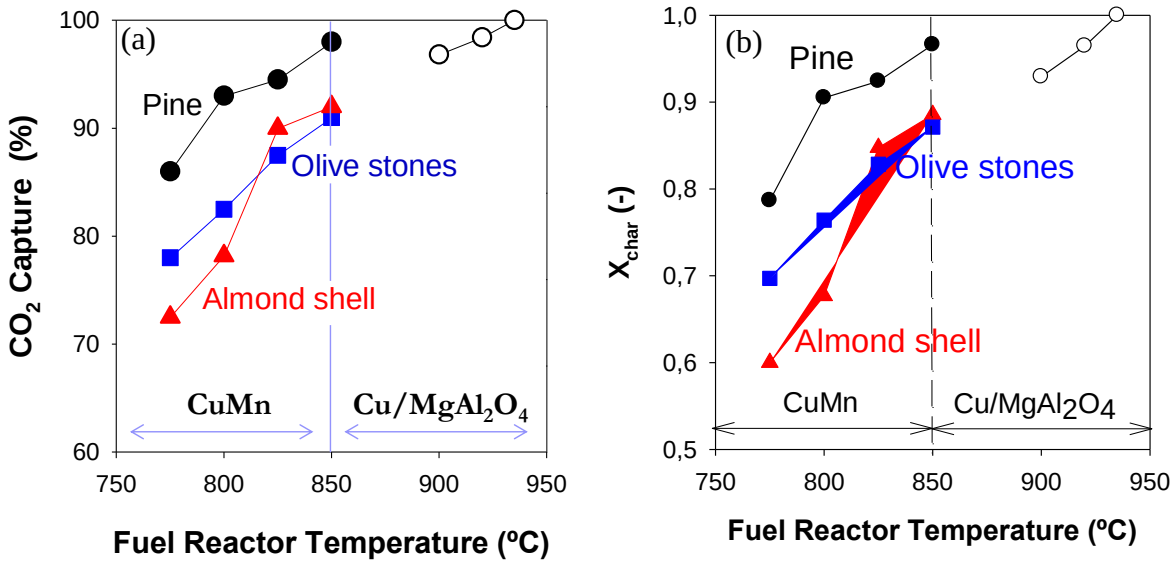

Figure 6. (a)CO_2 capture efficiency and; (b) char conversion, as a function of the fuel reactor temperature for the experiments carried out with Cu60MgAl and Cu34Mn66 oxygen carriers and three different biomasses: pine sawdust (●,○),almond shell (■) and olive stone (▲).

More in detail, the CO_2 capture efficiency increased from 86% to 95% with an increase of 50 ºC in the fuel reactor temperature with Cu33Mn66 and pine sawdust. When the fuel reactor temperature reached 850 ºC the value of the CO_2 capture efficiency increased to 98%. Regarding the CO_2 capture efficiency for almond shell and olive stone, it is lower than that obtained for the pine sawdust in the entire fuel reactor temperature interval studied. For both biomasses as well as in the case of the pine biomass, the CO_2 capture efficiency increases with the fuel reactor temperature, reaching values higher than 90%. The difference between char conversion for the different biomasses would be related with the difference in their char reactivity (Adánez-Rubio et al. 2018b). In addition, it can be seen that almond shells and olive stones have a larger amount of fixed carbon in their compositions; see Table 2. Therefore a larger amount of char will be produced in the fuel reactor which must be burned. Thus for biomasses with lower reactivity than the pine sawdust it would be necessary to increase the fuel reactor temperature or to install a carbon stripper (see Figure 1) to reduce the amount of unburnt char transferred to the air reactor and thus to increase the CO_2 capture efficiency over 95%. But as high CO_2 capture values were achieved with pine sawdust without the need of using a carbon separation system, the use of a carbon stripper could be avoided with this biomass.

In the case of the Cu-based oxygen carrier (Cu60MgAl) in Figure 5 it can be seen that, equal for Cu34Mn66, CO_2 capture efficiency increases with the fuel reactor temperature. Thus, with the pine sawdust high CO_2 capture efficiencies were found at fuel reactor temperatures higher than 900ºC, reaching 100% efficiency at 935ºC. As the temperature increases, the oxygen uncoupling effect increases. Thus, the O_2 equilibrium at 900ºC is 1.5 vol%. But what is more relevant is the high oxygen generation rate that the oxygen carrier shows at temperatures higher than 900ºC (Adánez-Rubio et al. 2012a). As a consequence, when the fuel reactor temperature increased, the rate of char combustion was directly increased, increasing the CO_2 capture efficiency (Adánez-Rubio et al. 2014a).

Comparing the results obtained for both oxygen carriers burning pine sawdust biomass, it can be seen in Figure 6 that the fuel reactor temperature is a key parameter to obtain high CO_2 capture efficiencies. With Cu60MgAl a 100% CO_2 capture efficiency was reached at 935 ºC. In the case of Cu34Mn66 it would predictible to reach a 100% of CO_2 capture around 865-875 ºC. So, it can be concluded that the Mn introduced in a Cu-based oxygen carrier reduces the operating temperature window in the fuel reactor mainteining the complete combustion to CO_2 and H_2O of the fuel. In addition, high CO_2 capture efficiency was achieved for high reactive biomass without the need of a carbon separation system; i.e. the carbon stripper could be avoided. However, for less reactive biomasses than pine sawdust, e.g. almond shell and olive stone, it would be necessary to increase the fuel reactor temperature over 875 ºC or to install a carbon stripper.

It is possible to compare the results obtained by CLOU process burning three different biomasses with the results obtained with *i*G-CLC process. Mendiara et al. (2017) did experiments in a 0.5 kW_{th} unit for *i*G-CLC process burning three different biomasses between 900 to 990 ºC. They found that at 900 ºC the CO_2 capture efficiency was around 90% for almond shells and olive stones and 96% for pine sawdust (920 ºC), like in CLOU process at 850 ºC. In the same study 100% CO_2 capture efficiency was obtained at 950ºC for all biomasses. However, looking for the combustion efficiency in the fuel reactor, in the case of the *i*G-CLC process at all temperatures the oxygen demand (that it is directly related with the combustion efficiency in the fuel reactor) was around 10-30% for the interval of temperatures studied. On the contrary, no gaseous unburnt products were found in the gas exit stream of the CLOU process experiments.

4 Conclusions

The operation with three different biomasses and two different CLOU oxygen carriers was carried out in a 1.5 kW_{th} CLOU system during 10 h using a Cu-based oxygen carrier (Cu60MgAl) and 65 h (40 h of combustion) using a Cu-Mn mixed oxide as oxygen carrier (Cu34Mn66). Gaseous unburnt compounds were not present in the fuel reactor outlet even at the lowest temperature studied (775 ºC) in the fuel reactor, being CO_2, H_2O and O_2 the only products of reaction for the three biomasses studied in this work. Using pine sawdust as fuel the CO_2 capture efficiency was higher than 95 % in most of the cases at operation temperatures in the fuel reactor as low as 850 ºC.

The oxygen release behavior of Cu60MgAl and Cu34Mn66 depends in different way of the temperature and different operating windows were found for the biomass combustion. For the Cu60MgAl operation window was from 900 to 935 ºC, while for Cu34Mn66 the operation window was form 775 to 850 ºC. The CO_2 capture efficiency was improved at higher temperatures for both oxygen carriers, reaching a CO_2 capture efficiency as high as 98 % at 850 ºC (Cu34Mn66) and 100% at 935ºC (Cu60MgAl). Therefore, the presence of a carbon separation system, e.g. the carbon stripper could be avoided when pine sawdust was used as fuel.

For almond shells and olive stones complete combustion was also obtained and the CO_2 capture efficiency increased with the fuel reactor temperature, reaching values higher than 90% at temperatures below 850 ºC with Cu34Mn66. As a function of the results obtained, for biomasses with lower reactivity than pine sawdust it would be necessary to increase the fuel reactor temperature or to install a carbon stripper to reduce the amount of unburnt char transferred to the air reactor and thereby to increase the CO_2 capture efficiency over 95%.

Acknowledgments

This work was supported by the Spanish Ministry of Economy and Competitiveness (MINECO Project: ENE2014-56857-R) and the European Union ERDF funds. I. Adánez-

Submitted, accepted and published by
Mitigation and Adaptation Strategies for Global Change (2019)
https://doi.org/10.1007/s11027-019-9840-5

Rubio acknowledges the MINECO and Universidad de Zaragoza (UZ) for the post-doctoral contract awarded (FJCI-2015-23862). A. Pérez-Astray thanks MINECO for the BES-2015-074651 pre-doctoral fellowship co-financed by the European Social Fund.

5 Notation

Symbols

F_i	Molar flow of compound *i* (mol/s)
M_i	Atomic or molecular mass of *i* elements or compound (kg/mol)
$\dot{m}_{SF}$	Mass flowrate of biomass fed in to the fuel reactor (kg/h)
m^*_{FR}	Specific solids inventory (kg/MW_{th})
$\dot{m}_s$	Solids circulation rate (kg/h)
R_{OC}	Oxygen transport capability (kg oxygen per kg of oxygen carrier)
$X_{char,FR}$	Char conversion (-)

Greek letters

ϕ	Oxygen carrier to fuel ratio (-)
η_{CC}	CO_2 capture efficiency (-)
$\eta_{comb,FR}$	Combustion efficiency in the fuel reactor (-)
Ω_{SF}	Stoichiometric mass of O_2 to convert 1 kg of biomass (kg/kg)

Subscripts

outAR	Outlet stream from air reactor
outFR	Outlet stream from fuel reactor

6 References

Abad A, Adánez-Rubio I, Gayán P, García-Labiano F, de Diego L, Adánez J (2012) Demonstration of chemical-looping with oxygen uncoupling (CLOU) process in a 1.5

kW_{th} continuously operating unit using a Cu-based oxygen-carrier International Journal of Greenhouse Gas Control 6:189-200

Abad A, Gayán P, de Diego LF, García-Labiano F, Adánez J (2018) Modelling Chemical-Looping assisted by Oxygen Uncoupling (CLaOU): Assessment of natural gas combustion with calcium manganite as oxygen carrier Proceedings of the Combustion Institute doi:10.1016/j.proci.2018.09.037

Adánez-Rubio I, Abad A, Gayan P, de Diego LF, Adánez J (2018a) CLOU process performance with a Cu-Mn oxygen carrier in the combustion of different types of coal with CO_2 capture Fuel 212:605-612

Adánez-Rubio I, Abad A, Gayán P, de Diego LF, García-Labiano F, Adánez J (2012a) Identification of operational regions in the Chemical-Looping with Oxygen Uncoupling (CLOU) process with a Cu-based oxygen carrier Fuel 102:634-645

Adánez-Rubio I, Abad A, Gayán P, de Diego LF, García-Labiano F, Adánez J (2013) Performance of CLOU process in the combustion of different types of coal with CO_2 capture International Journal of Greenhouse Gas Control 12:430-440

Adánez-Rubio I, Abad A, Gayán P, de Diego LF, García-Labiano F, Adánez J (2014a) Biomass combustion with CO_2 capture by chemical looping with oxygen uncoupling (CLOU) Fuel Processing Technology 124:104-114 doi:http://dx.doi.org/10.1016/j.fuproc.2014.02.019

Adánez-Rubio I, Abad A, Gayán P, García-Labiano F, de Diego LF, Adánez J (2014b) The fate of sulphur in the Cu-based Chemical Looping with Oxygen Uncoupling (CLOU) Process Applied Energy 113:1855-1862

Adánez-Rubio I, Gayan P, Abad A, de Diego LF, García-Labiano F, Adánez J (2017a) Coal combustion by a spray granulated Cu-Mn mixed oxide for CLOU process Applied Energy 208:561-570 doi:10.1016/j.apenergy.2017.09.098

Adánez-Rubio I, Gayán P, Abad A, de Diego LF, García-Labiano F, Adánez J (2012b) Evaluation of a Spray-Dried $CuO/MgAl_2O_4$Oxygen Carrier for the Chemical Looping with Oxygen Uncoupling Process Energy Fuels 26:3069-3081

Adánez-Rubio I, Gayán P, Abad A, García-Labiano F, de Diego LF, Adánez J (2014c) Kinetic analysis of a Cu-based oxygen carrier: Relevance of temperature and oxygen partial pressure on reduction and oxidation reactions rates in Chemical Looping with Oxygen Uncoupling (CLOU) Chemical Engineering Journal 256:69-84 doi:http://dx.doi.org/10.1016/j.cej.2014.06.102

Adánez-Rubio I, Izquierdo MT, Abad A, Gayan P, de Diego LF, Adánez J (2017b) Spray granulated Cu-Mn oxygen carrier for chemical looping with oxygen uncoupling (CLOU) process International Journal of Greenhouse Gas Control 65:76-85 doi:https://doi.org/10.1016/j.ijggc.2017.08.021

Adánez-Rubio I et al. (2018b) Chemical looping combustion of biomass: CLOU experiments with a Cu-Mn mixed oxide Fuel Processing Technology 172:179-186 doi:10.1016/j.fuproc.2017.12.010

Adánez J, Abad A, Mendiara T, Gayán P, de Diego LF, García-Labiano F (2018) Chemical looping combustion of solid fuels Progress in Energy and Combustion Science 65:6-66 doi:10.1016/j.pecs.2017.07.005

Council IOO (2017) http://www.internationaloliveoil.org

Fruit IND (2017) http://www.nutfruit.org

Garcia Labiano F, García Labiano F, de Diego L, Gayán P, Abad A, Adánez J (2013) Fuel reactor modelling in chemical-looping combustion of coal: 2—simulation and optimization Chemical Engineering Science 87:173-182

Gayán P, Abad A, de Diego LF, García-Labiano F, Adánez J (2013) Assessment of technological solutions for improving chemical looping combustion of solid fuels with CO_2 capture Chemical Engineering Journal 233:56-69 doi:10.1016/j.cej.2013.08.004

IPCC (2014) Climate Change 2014: Synthesis Report. Contribution of Working Groups I, II and III to the Fifth Assessment Report of the Intergovernmental Panel on Climate Change; Geneva (Switzerland):151

Mattisson T, Lyngfelt A, Leion H (2009) Chemical-looping with oxygen uncoupling for combustion of solid fuels International Journal of Greenhouse Gas Control 3:11-19

Mendiara T, Adánez-Rubio I, Gayán P, Abad A, de Diego LF, García-Labiano F, Adánez J (2016) Process Comparison for Biomass Combustion: In Situ Gasification-Chemical Looping Combustion (iG-CLC) versus Chemical Looping with Oxygen Uncoupling (CLOU) Energy Technology 4:1130-1136 doi:10.1002/ente.201500458

Mendiara T, García-Labiano F, Abad A, Gayán P, de Diego LF, Izquierdo MT, Adánez J (2018) Negative CO_2 emissions through the use of biofuels in chemical looping technology: A review Applied Energy 232:657-684 doi:https://doi.org/10.1016/j.apenergy.2018.09.201

Mendiara T et al. (2017) Chemical Looping Combustion of different types of biomass in a 0.5 kW_{th} unit Fuel Submitted

Schmitz M, Linderholm CJ (2016) Performance of calcium manganate as oxygen carrier in chemical looping combustion of biochar in a 10 kW pilot Applied Energy 169:729-737 doi:10.1016/j.apenergy.2016.02.088

Simell P, Ståhlberg P, Kurkela E, Albrecht J, Deutsch S, Sjöström K (2000) Provisional protocol for the sampling and anlaysis of tar and particulates in the gas from large-scale biomass gasifiers. Version 1998 Biomass and Bioenergy 18:19-38

Wang X et al. (2017) CuO supported on olivine as an oxygen carrier in chemical looping processes with pine sawdust used as fuel Chemical Engineering Journal 330:480-490 doi:10.1016/j.cej.2017.07.175